Two-Dimensional Fourier Transform Raman Correlation Spectroscopy Studies of Polymer Blends: Conformational Changes and Specific Interactions in Blends of Atactic Polystyrene and Poly(2,6-dimethyl-1,4-phenylene ether)

Yanzhi Ren,[†] Tsuyoshi Murakami,[‡] Toshikatsu Nishioka,[‡] Kenichi Nakashima,[§] Isao Noda,[⊥] and Yukihiro Ozaki*[,†]

Department of Chemistry, School of Science, Kwansei Gakuin University, Nishinomiya 662-8501, Japan, Idemitsu Petrochemical Co., Ltd., 1-1, Anesaki-Kaigan, Ichihara 299-0193, Japan, Department of Chemistry, Faculty of Science and Engineering, Saga University, Saga 849-8502, Japan, and The Procter and Gamble Company, Miami Valley Laboratories, PO Box 538707, Cincinnati, Ohio 45253-8707

Received January 20, 1999; Revised Manuscript Received June 3, 1999

ABSTRACT: Fourier transform (FT) Raman spectra have been measured for atactic polystyrene (PS), poly(2,6-dimethyl-1,4-phenylene ether) (PPE) and their blends of different compositions: PS/PPE = 90/10, 70/30, 50/50, 30/70, 10/90. Composition-dependent spectral variations of the blends have been analyzed by generalized two-dimensional (2D) correlation spectroscopy to study the conformational changes and specific interactions in the blends. The FT-Raman spectra have been divided into two sets for the 2D correlation: set A of high PS contents (PS/PPE = 100/0, 90/10, 70/30) and set B of high PPE contents (PS/PPE = 50/50, 30/70, 10/90). The 2D synchronous correlation analysis discriminates between the bands of PS and those of PPE and detects bands that are not readily identifiable in the one-dimensional spectra of PS and PPE. The main chain conformation of PS undergoes a drastic change when mixed with PPE, as reflected in the abnormal behavior of bands at 1448 and 1329 cm^{-1} due to the backbone methylene vibrations and of the band at 1070 cm^{-1} due to the C−C stretching vibration. The 2D asynchronous correlation analysis reveals many out-of-phase band variations showing opposite trends in set A and set B. Bands at 1614, 1590, 1378, 1305, 1131, 1112, 1093, 1004, 572, and 241 cm^{-1} due to PPE and those at 1602, 1031, 1000, and 202 cm^{-1} due to PS are found to be indicative of the specific interaction common to set A and set B. It also reveals bands that are unique to the particular molecular interactions in set A or set B: 1606 cm^{-1} for set A and 1309 cm^{-1} for set B. It is concluded from the asynchronous spectra that not only the phenyl rings of PS and PPE but also the CH_3 groups of PPE play important roles in the formation of the blends.

Introduction

Generalized two-dimensional (2D) correlation spectroscopy,[1] which is an extension of the original 2D correlation spectroscopy proposed by Noda in 1986,[2−4] has received great attention in recent years. The new 2D method can handle spectral fluctuations as an arbitrary function of time or any other physical variables such as temperature, pressure, concentration, and composition. Generalized 2D correlation spectra emphasize spectral features not readily observable in conventional one-dimensional spectra. It helps to probe the specific order of certain spectral events taking place with the development of a controlling physical variable.

A number of research groups have reported applications of generalized 2D correlation spectroscopy.[5−20] Some applications are concerned with temperature-dependent spectral variations[7,9−12,14,15,18,19] and others discuss concentration-dependent spectral changes.[13,20] 2D near-infrared (NIR) and mid-infrared (MIR) heterospectral correlation analysis were also reported.[18,19] In this paper we present a 2D NIR excited Fourier transform (FT) Raman correlation spectroscopic study on polymer blends.

Raman spectroscopic studies of polymers have recently been revitalized with the introduction of NIR excited FT-Raman and multichannel spectroscopy.[21−23] In the past, it was often difficult to measure Raman spectra from material samples of practical importance such as blends, degraded specimens, and heat-treated samples, since fluorescence from these specimens was very severe.[24] The specimen had to be carefully selected or purified. The advantage of NIR excitation is that fluorescence from a polymer sample is minimized. With the advent of NIR FT-Raman spectroscopy, almost all kinds of polymer samples can be subjected to Raman measurements. The Raman technique also enables us to measure vibrational spectra of polymer blends originally in the form of pellets. While the infrared technique can also yield vibrational spectra of polymer blends, the blends in pellets have to be cast or hot-pressed into thin films of tens of micrometers for the infrared measurements, thereby losing their original structures.[24−26]

Vibrational spectroscopic studies on polymer blends have been largely restricted to those containing hydrogen bonds and have mainly used infrared spectroscopy.[26−29] Hydrogen bonds are often employed to enhance the miscibility in polymer blends,[30,31] and infrared spectroscopy is powerful in investigating hydrogen bonds.[30] In contrast, vibrational spectroscopic studies on the specific interactions in polymer blends without hydrogen bonding have been less often reported.

* To whom correspondence should be addressed. Fax: +81-798-51-0914. E-mail: ozaki@kwansei.ac.jp.
[†] Kwansei-Gakuin University.
[‡] Idemitsu Petrochemical Co., Ltd.
[§] Saga University.
[⊥] The Procter and Gamble Co.

10.1021/ma990072e CCC: $18.00
Published on Web 08/24/1999

Scheme 1

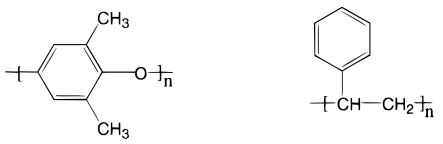

PPE PS

Wellinghoff et al.[32] reported a UV−visible study of the phenyl ring of PPE and an infrared study of the ether bond of PPE in PS/PPE blends. The lack of vibrational literature about polymer blends without hydrogen bonds may be due to the difficulty in identifying spectral signatures for the specific interactions between the component polymers. Generalized 2D FT-Raman correlation spectroscopy, which identifies various intra- and intermolecular interactions through selective correlation of bands,[1] may be able to pick up the characteristic features for the specific interaction in polymer blends.

In the present study, generalized 2D FT-Raman correlation spectroscopy has been applied to explore the intermolecular interactions without hydrogen bonding in blends of atactic polystyrene (PS) and poly(2,6-dimethyl-1,4-phenylene ether) (PPE) (Scheme 1). PS and PPE are well-known to be compatible at the molecular level without any hydrogen-based miscibility enhancers.[32−37] Wellinghoff et al.[32] claimed that the dispersion interaction between the phenyl ring of PS and that of PPE is responsible for the blend compatibility. It was reported that a change in the shape of an infrared band of PPE at 1188 cm^{-1} due to the C−O−C stretching vibration is an evidence for this interaction.[32] On the other hand, on the basis of NMR measurements of the blends, Djordjevic and Porter[37] suggested that the specific interaction between the methyl groups of PPE and the phenyl ring of PS plays an important role in the compatibility between PS and PPE. Therefore, there is a controversy over the origin of the compatibility of the blend system.

Generalized 2D correlation analysis requires a series of perturbation-dependent spectra. In the present case, they are obtained by varying the composition of the blends of PS and PPE. FT-Raman spectra were measured for PS, PPE, and their blends of five different compositions; i.e., PS/PPE = 90/10, 70/30, 50/50, 30/70, and 10/90. The PS/PPE blends of different compositions have different mechanical behaviors, implying different molecular environments and intermolecular interactions.[33−36] The blends with PS content in the range of 100−70% are brittle materials, which craze over a large temperature regime; those with PS content in the range of 70−50% are a ductile glass, which deforms by microshear processes. To investigate the detailed structural features in the blends by 2D correlation analysis, the FT-Raman spectra have been divided into two sets: set A of high PS content and set B of high PPE content. Set A contains three spectra: those of PS/PPE = 100/0, 90/10, and 70/30. Set B contains three spectra: those of PS/PPE = 50/50, 30/70, and 10/90. The present 2D FT-Raman correlation analysis shows that it is feasible to analyze the structure of polymer blends even with only a handful of composition-dependent spectra.

Experimental Section

A high molecular weight atactic PS (M_w = 240 000, M_n = 112 000; Idemitsu Petrochemical Co., Ltd.) was mixed with additive-free PPE (M_w = 36 300, M_n = 13 200) at 280 °C. The PS was proved to be atactic by both FT-IR and FT-Raman measurements.

The NIR excited FT-Raman spectra of the PS/PPE blends were measured at a 4 cm^{-1} resolution with a JEOL JRS−FT6500N Raman spectrometer equipped with an InGaAs detector. The excitation source used was the 1064 nm line from a cw Nd:YAG laser (Spectron SL301). The laser power at the sample position was typically 500 mW. Raman scattered light was collected with a 180° backscattering geometry, and all the spectra were the results of the co-addition of 400 interferograms.

PPE was obtained as powder while PS and its blends with PPE were provided as pellets. In general, the baselines of FT-Raman spectra depend on the conditions and forms of samples. In the present case, the baseline of the FT-Raman spectrum of PPE in the powder form is somewhat different from that of the spectra of the rest in the pellets, so that the spectrum of PPE was excluded for the 2D correlation analysis. The spectra of PS and its blends with PPE were divided into two sets, as described in the Introduction. All the spectra employed in the 2D correlation analysis were normalized. The spectra in set A were arranged in the following order: PS → SE91 (90% PS plus 10% PPE) → SE73 (70% PS plus 30% PPE). Those in set B were arranged in the following order: SE55 (50% PS plus 50% PPE) → SE37 (30% PS plus 70% PPE) → SE19 (10% PS plus 90% PPE).

For the 2D correlation analysis we used a piece of software named "2D Pocha", which was composed by Daisuke Adachi (Kwansei Gakuin University). The one-dimensional reference spectra shown at the side and top of the 2D correlation maps are the average over three spectra in one set. In the 2D correlation maps regions without dots indicate positive correlation intensities, while regions with dots indicate negative correlation intensities.

Results and Discussions

The FT-Raman spectra of PS, PPE and their blends with different compositions are shown in Figure 1. Assignments of the Raman bands of PS and PPE are listed in Table 1 and 2, respectively. The assignments are based upon refs 38−40. The Raman bands of PPE below 572 cm^{-1} are not included in Table 2. They are assigned roughly to various ring deformation modes.

1. Interaction Spectra Of PS/PPE Blends. The specific interactions in polymer blends have long been studied in terms of the "interaction spectrum".[24,30] The interaction spectrum of a blend is obtained by subtracting the spectra of the component polymers in the pure form from the blend spectrum, thus representing only the net interaction between the component polymers. The concept of the interaction spectrum has been effective in studying the specific interactions in polymer blends with hydrogen bonds.

The interaction spectrum of a polymer blend can be obtained either by manual subtraction or an autosubtraction scheme provided by a piece of popular commercial software, such as Grams/386, version 3.02. (The Galactic Industries Corp.). Using a simple autosubtraction scheme, only the interaction spectrum of SE91 can be clearly obtained, while the meaningful interaction spectra of other blends could not be obtained.

However, the interaction spectra of all the blends can be obtained by careful manual subtraction. It is seen from Figure 1 that the strongest band of PPE is located at 572 cm^{-1}, and that of PS appears at 1000 cm^{-1}. When the PS or PPE spectrum is subtracted from a blend spectrum, the subtraction factor is adjusted such that the band at 1000 or 572 cm^{-1} disappears. In the case of a doublet of bands which are separated by only 4 cm^{-1} (the resolution) occur, the subtraction factor is chosen

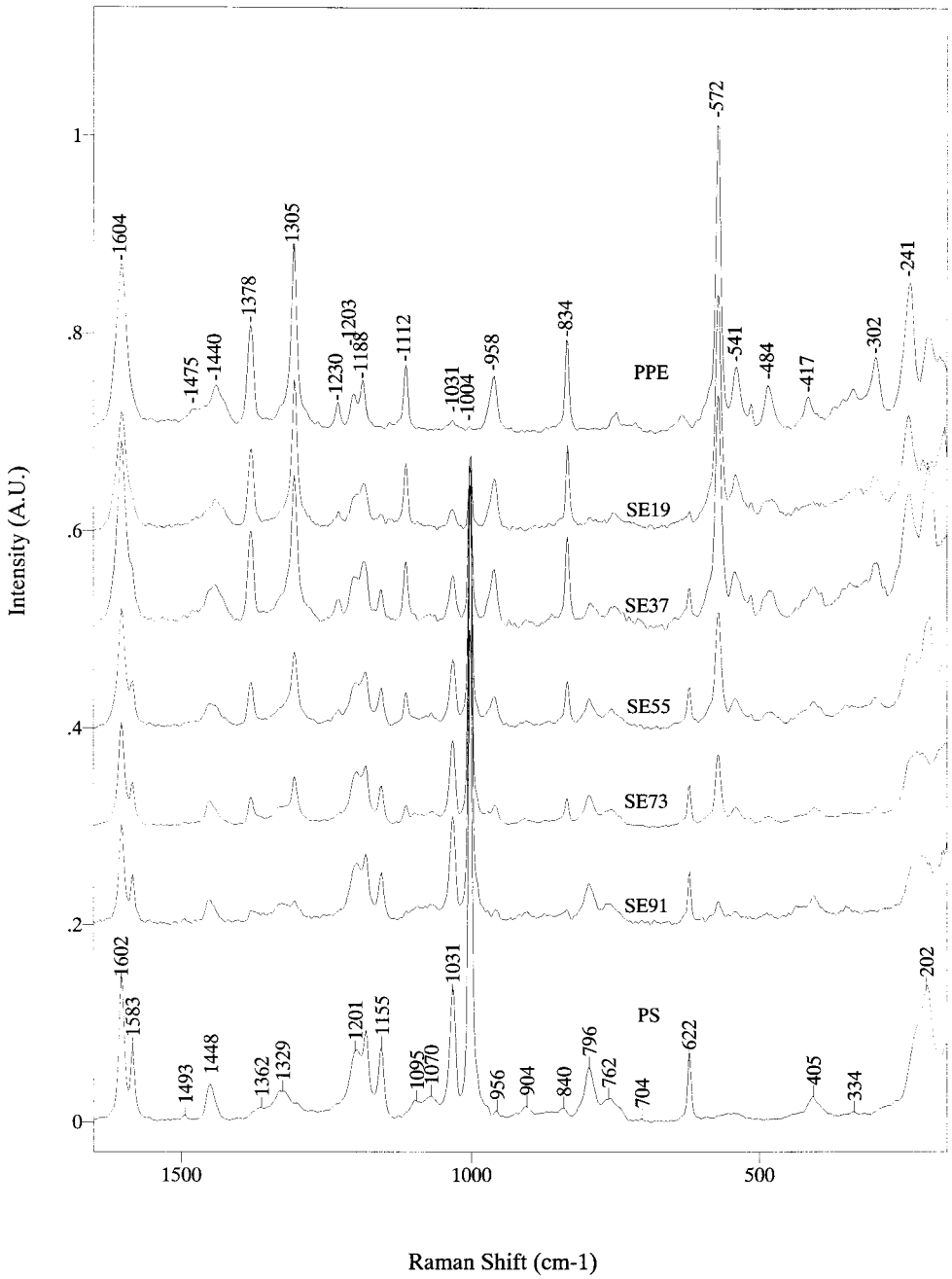

Figure 1. FT-Raman spectra of PS, PPE and their blends of different compositions (PS/PPE = 90/10, 70/30, 50/50, 30/70, 10/90).

such that the downward peak is as intense as the upward peak. For example, the interaction spectrum of SE91 is obtained as follows. First, we subtract the PPE spectrum from the SE91 spectrum such that the band at 572 cm^{-1} disappears. Then, we subtract the PS spectrum from the resulting spectrum such that the peak at 1000 cm^{-1} is as intense as the peak at 1004 cm^{-1}, as shown in Figure 2(1).

Of note in Figure 2 is that the phenyl ring-stretching vibrations (ν_8) of PS and PPE appear strongly in the interaction spectra of all the blends. The bands at 1602 and 1583 cm^{-1} are assigned to the monosubstituted phenyl ring of PS, while the band at 1590 cm^{-1} is assigned to the tetrasubstituted phenyl ring of PPE. (These assignments come from the following 2D analysis.) The phenyl ring-stretching vibrations can be influenced only by strong interactions. Therefore, the bands at 1602, 1583, and 1590 cm^{-1} in Figure 2 are indicative of the specific interaction in the blends. It seems very likely that the phenyl rings of PS and PPE are involved in the formation of the blends.

Noticeably, the band at 1590 cm^{-1} is discernible only for SE37, indicating that the specific interaction in SE37 is different from that in other blends. The band at 1583 cm^{-1} is discernible only for SE91 and SE73. Hence, the specific interaction in SE91 and SE73 may be different from that in other blends. This can serve as an account for our division of the PS/PPE blends into set A and set B. The other phenyl ring-stretching bands are found at 1309 and 1305 cm^{-1} in Figure 2. The band at 1309 cm^{-1} should be of the same origin as the band at 1305 cm^{-1}. The doublet at 1309 and 1305 cm^{-1} is discernible for the blends in set B, i.e., SE55, SE37, and SE19. Therefore, the bands at 1305 and 1309 cm^{-1} are indicative of the specific interaction in set B. This conclusion can also be drawn from the following 2D correlation analysis.

Table 1. Assignments of the Bands in the FT-Raman Spectrum of PS

frequency (cm^{-1})	intensity[a]	assignments (Wilson no.)[b]
1602	s	ring str (8a)
1583	m−s	ring str (8b)
1493	vw	ring str (19a)
1448	m−s	CH_2 bend
1362	w	CH_2 wag
1329	m	CH_2 wag
1201	m−s	in-plane CH def
1181	m−s	in-plane CH def
1155	m−s	in-plane CH def (15)
1095	w	in-plane CH def (18b)
1070	w	skeletal C−C str
1031	s	in-plane CH def (18a)
1000	vs	in-plane ring def + out-of-plane CH def (12 + 5)
956	vw	out-of-plane CH def (17a)
904	w	out-of-plane CH def (17b)
840	w	out-of-plane CH def
796	m−s	out-of-plane CH bend (10a)
762	m	ring str (1)
704	vw	out of plane ring def (4)
622	m−s	in-plane ring def (6b)
543	vw	out-of-plane ring def (16b)
405	w−m	C−C−C bend +out-of-plane ring def (16a)
334	vw	C−C−C bend + in-plane CH def (9b)
202	vs	out-of-plane ring def

[a] Key: vs, very strong; s, strong; m, medium; w, weak; vw, very weak. [b] Key: def, deformation; str, stretching; bend, bending; wag, wagging

Table 2. Assignments of the Bands in the FT-Raman Spectrum of PPE[a]

frequency (cm^{-1})	intensity	assignment (Wilson no.)
1604	s	ring str (8a)
1475	m	ring str (19a)
1440	m	CH_3 asym def
1378	s	CH_3 sym def.
1305	s	ring str (14)
1230	m	aryl-O band
1203	m	in-plane CH def
1188	m	in-plane CH def
1112	m	in-plane CH def (18b)
1031	w	in-plane CH def (18a)
1004	vw	in-plane ring def (12)
958	m	out-of-plane CH def
572	vs	out-of-plane ring def

[a] The phenylene ring of PPE is tetrasubstituted at the 1-, 2-, 4-, and 6-positions. Like the phenyl ring of PS, it also has $C_{2v}{}^{y}$ symmetry.

Apart from the ring-stretching vibrations, aromatic ring deformation modes are generally not affected by weak interactions. Bands at 229 and 202 cm^{-1} due to out-of-plane ring deformations are indicative of the specific interaction in the blends. The band at 229 cm^{-1} is observable only for the blends of set B, and thus, is unique to the specific interaction in set B. The same conclusion can also be reached from the 2D correlation analysis. Other ring deformation vibrations are found at 1004, 1000, 622, 572, 541, 486, and 302 cm^{-1} in Figure 2. The following 2D correlation analysis will show that these bands are also signs for the specific interaction in the PS/PPE blends.

The aromatic CH deformation bands of polymers are known to be influenced by many factors, including the specific interactions, polymer conformation changes, and other subtle changes in the chemical environment. In Figure 2, bands at 1155, 1031, 1112, 958, and 834 cm^{-1} are assigned to the CH deformations of the phenyl rings of PS and PPE. Their appearance in the interaction spectra may have many implications. According to the following 2D analysis, the PS band at 1031 cm^{-1} and the PPE band at 1112 cm^{-1} indicate the specific interaction in the PS/PPE blends. On the other hand, the band at 1155 cm^{-1} due to PS and the bands at 958 and 834 cm^{-1} due to PPE are indicative of conformation changes in PS and PPE, respectively. Such detailed assignments are not yet possible from the simple interaction spectra.

The methylene bands of PS and the methyl band of PPE may also be influenced by many factors. A band at 1448 cm^{-1} is mainly due to a CH_2 scissoring mode of PS. While the semicircle stretching mode of the aromatic ring is also located at this wavenumber, it is relatively weak and insensitive to the conformation change of PS. A band at 1378 cm^{-1} is assigned to a CH_3 deformation mode of PPE. The following 2D correlation analysis suggests that the methylene band is subject to the conformation change of PS, while the methyl band is indicative of the specific interaction in the PS/PPE blends.

As a summary, the traditional approach of investigating the interaction spectra can yield some information about the specific interaction in the PS/PPE blends. The accuracy of these information relies on the arbitrary choice of particular bands, on which the manual subtraction has been based. The best way is to choose strong bands that are insensitive to polymer blending. However, the strong bands of PS and PPE are all sensitive to the specific interaction and conformation changes of the component polymers. The manual subtraction results are as arbitrary as the choice of the band at 1000 cm^{-1} for PS and the band at 572 cm^{-1} for PPE. At this point, 2D correlation analysis has the advantage that the structural information derived therefrom does not depend on any arbitrary choice of particular bands.

2. Background for 2D Correlation Analysis of Polymer Blends. The 2D FT-Raman study of the blends of PS and PPE has dual purposes. One is to separate the bands of PS from those of PPE in the spectra of the blends. Another is to study the specific interaction between PS and PPE in the blends. The first purpose is realized by synchronous 2D correlation analysis of the FT-Raman spectra. The intensities of the bands of PS are decreasing while those of PPE are increasing for both set A and set B. Using Φ to designate synchronous 2D correlation intensities between two bands, we have the following relations:

$$\Phi[\nu(\mathrm{PS}), \nu(\mathrm{PS})] > 0,\ \Phi[\nu(\mathrm{PPE}), \nu(\mathrm{PPE})] > 0,\ \Phi[\nu(\mathrm{PS}), \nu(\mathrm{PPE})] < 0,\ \text{and}\ \Phi[\nu(\mathrm{PPE}), \nu(\mathrm{PS})] < 0$$

On the basis of these relations, we are able to ascribe bands in the spectra of the blends to PS or PPE.

The second goal is realized by asynchronous 2D correlation analysis of the FT-Raman spectra. An asynchronous correlation peak $\Psi[\nu_1, \nu_2]$ appears only if the intensity change of two bands at ν_1 and ν_2 has basically dissimilar or uncoordinated trends. In other words, the bands at ν_1 and ν_2 vary out-of-phase. In this paper, the appearance of any asynchronous peak can only be ascribed to structural changes in the blends of PS/PPE. The composition change in the blends causes band intensity changes that are proportional to the weight percentage of the component polymer. Such simple proportional changes alone do not give rise to asynchronous peaks.

The sign of an asynchronous correlation peak $\Psi[\nu_1, \nu_2]$ gives information about the sequential order of intensity change between two bands at ν_1 and ν_2.

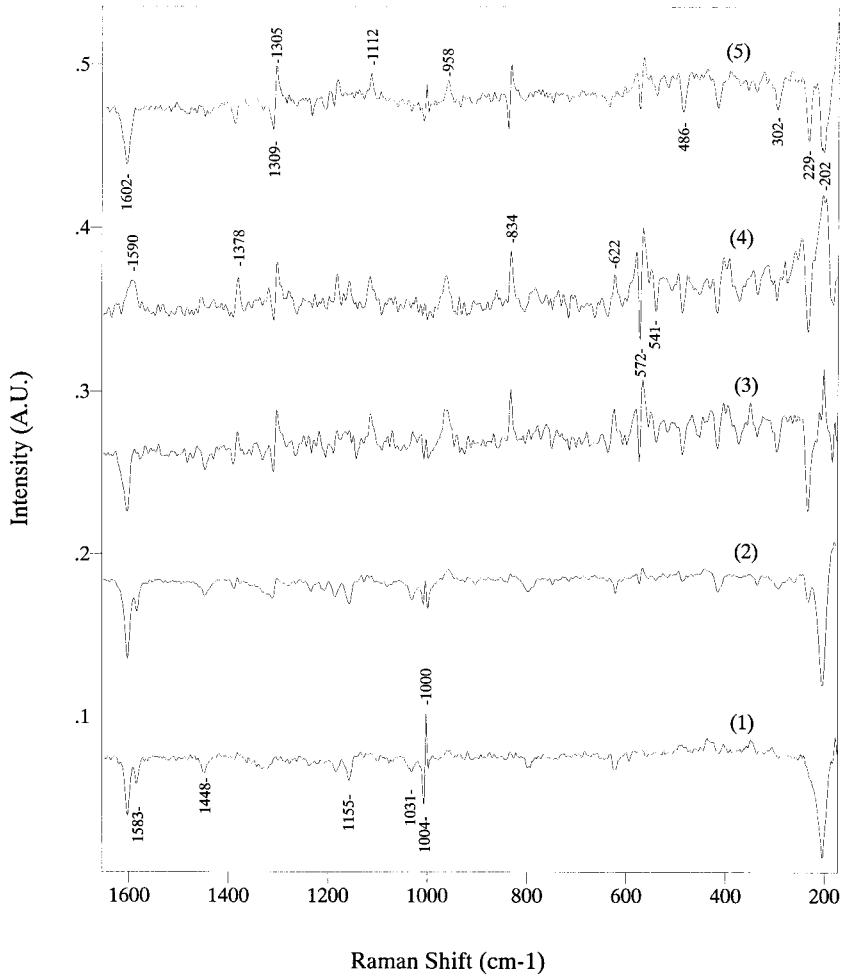

Figure 2. Interaction spectra of PS/PPE blends obtained by manually subtracting the FT-Raman spectra of PS and PPE from the spectra of the blends: (1) SE91; (2) SE73; (3) SE55; (4) SE37; (5) SE19.

According to Noda,[1] $\Phi[\nu_1, \nu_2] < 0$ and $\Psi[\nu_1, \nu_2] > 0$ imply that the intensity change at ν_1 occurs at higher PPE content compared to that at ν_2. So do $\Phi[\nu_1, \nu_2] > 0$ and $\Psi[\nu_1, \nu_2] < 0$. $\Phi[\nu_1, \nu_2] < 0$ and $\Psi[\nu_1, \nu_2] < 0$ imply that the intensity change at ν_1 takes place at lower PPE content than that at ν_2. So do $\Phi[\nu_1, \nu_2] > 0$ and $\Psi[\nu_1, \nu_2] > 0$. In this paper, we shall use these relationships to determine the sequential order of intensity change between two bands.

The aromatic ring-stretching and deformation modes of PS and PPE are affected only by strong interactions such as the specific interaction between PS and PPE, while aryl CH vibrations are affected by many factors such as simple conformational change and subtle change in the chemical environment. We shall ascribe any asynchronicity between the phenyl ring-stretching and deformation bands to the specific interaction between PS and PPE. However, one must take extra care in ascribing an asynchronicity $\Psi[\nu_1, \nu_2]$ between aryl CH vibrations to the specific interaction. The asynchronicity between two aryl CH vibrations is usually attributed to the conformation changes in the polymer blends, except for the following case. If the sequential order between ν_1 and ν_2 in set A is opposite to that in set B, then the bands at ν_1 and ν_2 can be regarded as indicative of the specific interaction between PS and PPE. This point needs a more detailed explanation. The specific interaction between PS and PPE is relatively weak in blends SE91 and SE19, and reaches the strongest when the PPE content is in the range of 30−50%.[33−36] With the increase in the PPE content from 0% to 90%, the spectral variations resulting from the specific interaction first experience increase, then decrease. This means that the sequential order between ν_1 and ν_2 has opposite trends for set A (from SE91 to SE73) and set B (from SE37 to SE19). If the intensity variation at ν_1 occurs before (after) that at ν_2 in set A, it will take place after (before) that at ν_2 in set B. In fact, asynchronous relationships which are common to set A and set B are always found to have opposite trends in the two sets. In the following discussion, the above features will be employed to ascribe an asynchronous peak either to the conformation change of the component polymers or to the specific interaction between them.

3. 2D Correlation Spectra of Set A. Figure 3A shows the 2D synchronous FT-Raman correlation spectrum of set A in the range of 1620−1290 cm^{-1}. The band at 1583 cm^{-1} is due to the monosubstituted phenyl ring of PS. According to the rule described above, the positive cross-peak at (1602, 1583 cm^{-1}) implies that the band at 1602 cm^{-1} is due to PS. The negative cross-peaks at (1378, 1583 cm^{-1}) and (1305, 1583 cm^{-1}) suggest that the bands at 1378 and 1305 cm^{-1} arise from PPE, as can be seen from Figure 1 and Table 2. Because of the positive correlation with the bands at 1378 and 1305 cm^{-1}, the bands at 1590 and 1614 cm^{-1} are assigned to PPE. Similarly, the bands at 1475 and 1428 cm^{-1} are determined to be due to PPE.

Table 3. Synchronous, Asynchronous 2D Correlation Intensities and the Order of Intensity Variations between Two Bands for Set A in the Ranges of 1620−1290 and 1220−1020 cm^{-1}

no.	Φ	Ψ	assignment	order[a]
1	Φ(1614, 1602) < 0	Ψ(1614, 1602) > 0	(PPE, PS)	1614 after 1602 cm^{-1}
2	Φ(1590, 1602) < 0	Ψ(1590, 1602) > 0	(PPE, PS)	1590 after 1602 cm^{-1}
3	Φ(1305, 1602) < 0	Ψ(1305, 1602) > 0	(PPE, PS)	1305 after 1602 cm^{-1}
4	Φ(1305, 1583) < 0	Ψ(1305, 1583) > 0	(PPE, PS)	1305 after 1583 cm^{-1}
5	Φ(1378, 1602) < 0	Ψ(1378, 1602) > 0	(PPE, PS)	1378 after 1602 cm^{-1}
6	Φ(1378, 1583) < 0	Ψ(1378, 1583) > 0	(PPE, PS)	1378 after 1583 cm^{-1}
7	Φ(1606, 1583) > 0	Ψ(1606, 1583) > 0	(?, PS)	1606 before 1583 cm^{-1}
8	Φ(1305, 1448) < 0	Ψ(1305, 1448) > 0	(PPE, PS)	1305 after 1448 cm^{-1}
9	Φ(1131, 1031) < 0	Ψ(1131, 1031) < 0	(PPE, PS)	1131 before 1031 cm^{-1}
10	Φ(1112, 1031) < 0	Ψ(1112, 1031) < 0	(PPE, PS)	1112 before 1031 cm^{-1}
11	Φ(1093, 1031) < 0	Ψ(1093, 1031) < 0	(PPE, PS)	1093 before 1031 cm^{-1}
12	Φ(1093, 1155) < 0	Ψ(1093, 1155) < 0	(PPE, PS)	1093 before 1155 cm^{-1}
13	Φ(1155, 1031) > 0	Ψ(1155, 1031) > 0	(PS, PS)	1155 before 1031 cm^{-1}

[a] ν_1 after (before) ν_2 means the intensity change of the band at ν_1 occurs at higher (lower) PPE contents than that at ν_2.

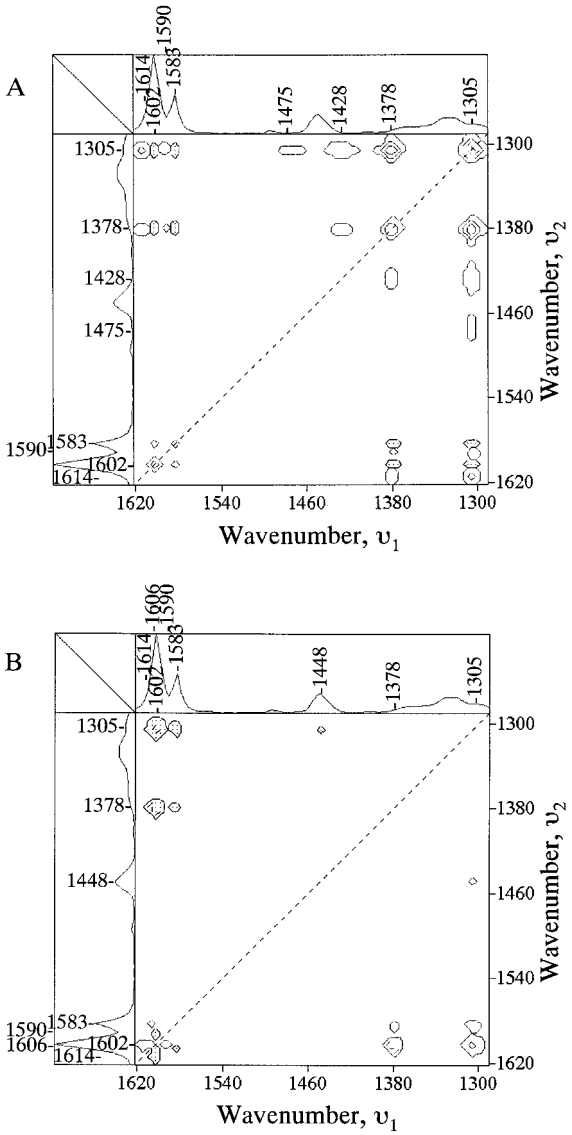

Figure 3. Synchronous (A) and asynchronous (B) 2D FT-Raman correlation spectra in the range 1620−1290 cm^{-1}, constructed from the spectra of PS, SE91, and SE73 (set A).

The 2D correlation analysis is powerful in separating bands of PS from those of PPE. In the region of 1620−1580 cm^{-1}, the bands due to ν_8 modes of PS and PPE are highly overlapped, but generalized 2D correlation analysis can pick up the bands due to PS and PPE separately from the spectra of the blends. It predicts the existence of two bands for PPE: one at 1614 cm^{-1} (ν_{8a}) and another at 1590 cm^{-1} (ν_{8b}). In Figure 1 only one band is identified around 1604 cm^{-1} in the spectrum of PPE.

It is seen from Figure 1 and Table 1 that the bands at 1448 and 1329 cm^{-1} due to PS have moderate intensities. However, neither autopeaks nor cross-peaks appear for them in Figure 3A. With the decrease of PS content in the blends, these bands due to PS should have occasional increase, instead of monotonic decrease (otherwise synchronous peaks would appear for them). In fact, in the one-dimensional spectra the intensity of the band at 1448 cm^{-1} is found to be 0.02922, 0.02426, and 0.02836 for PS, SE91, and SE73, respectively. The intensity of the band at 1329 cm^{-1} is read to be 0.02433, 0.02182, and 0.02388 for PS, SE91, and SE73, respectively. The bands at 1448 and 1329 cm^{-1} are due to methylene vibrations along the main chain. Thus, with the increase of PPE content in the blends the main chain conformation of PS undergoes some changes.

The corresponding asynchronous correlation spectrum is shown in Figure 3B. Asynchronicity is found between bands due to PS and PPE. The order of intensity variation between two bands is listed in Table 3. The first to fourth rows of Table 3 show that the intensity change of the bands at 1614, 1590, and 1305 cm^{-1} due to the ring-stretching modes of PPE occurs predominantly at higher PPE contents, in comparison with that of the bands at 1602 and 1583 cm^{-1} due to the ring-stretching modes of PS. The intensity change of these ring-stretching bands reveals the specific interaction between the phenyl rings of PS and PPE. Since these ring-stretching vibrations are influenced only by strong interactions, the specific interaction should be considerably favorable. This may explain the compatibility of PS and PPE at the molecular level.

The fifth and sixth rows of Table 3 are concerned with the asynchronicity between the band at 1378 cm^{-1} due to the methyl symmetric deformation of PPE and the bands at 1602 and 1583 cm^{-1} due to PS. In combination with the above results, it is seen that both the methyl groups and the aromatic rings of PPE and PS are involved in the formation of PS/PPE blends. This conclusion is different from the conclusion by Wellinghoff et al. that only the aromatic rings of PS and PPE are responsible for the compatibility of the blend.[32] Our conclusion is also not in agreement with the conclusion reached by Djordjevic et al. that it is the methyl groups of PPE and the aromatic ring of PS that are major cause for the miscibility of the blend.[37]

The band at 1606 cm^{-1} (the seventh row of Table 3) appears in Figure 3B and does not appear in Figure 3A

Table 4. Synchronous, Asynchronous 2D Correlation Intensities and the Order of Intensity Variations between Two Bands for Set A in the Ranges of 1020−780 and 650−190 cm^{-1}

no.	Φ	Ψ	assignment	order[a]
1	Φ(958, 1000) < 0	Ψ(958, 1000) < 0	(PPE, PS)	958 before 1000 cm^{-1}
2	Φ(834, 1000) < 0	Ψ(834, 1000) < 0	(PPE, PS)	834 before 1000 cm^{-1}
3	Φ(796, 1000) > 0	Ψ(796, 1000) > 0	(PS, PS)	796 before 1000 cm^{-1}
4	Φ(996, 1000) > 0	Ψ(996, 1000) > 0	(PS, PS)	996 before 1000 cm^{-1}
5	Φ(1004, 1000) > 0	Ψ(1004, 1000) > 0	(PPE, PS)	1004 before 1000 cm^{-1}
6	Φ(572, 202) < 0	Ψ(572, 202) > 0	(PPE, PS)	572 after 202 cm^{-1}
7	Φ(541, 202) < 0	Ψ(541, 202) > 0	(PPE, PS)	541 after 202 cm^{-1}
8	Φ(302, 202) < 0	Ψ(302, 202) > 0	(PPE, PS)	302 after 202 cm^{-1}
9	Φ(241, 202) < 0	Ψ(241, 202) > 0	(PPE, PS)	241 after 202 cm^{-1}
10	Φ(484, 572) > 0	Ψ(484, 572) > 0	(PPE, PPE)	484 before 572 cm^{-1}
11	Φ(430, 572) > 0	Ψ(430, 572) > 0	(PPE, PPE)	430 before 572 cm^{-1}
12	Φ(349, 572) > 0	Ψ(349, 572) > 0	(PPE, PPE)	349 before 572 cm^{-1}
13	Φ(302, 572) > 0	Ψ(302, 572) > 0	(PPE, PPE)	302 before 572 cm^{-1}

[a] ν_1 after (before) ν_2 means the intensity change of the band at ν_1 occurs at higher (lower) PPE contents than that at ν_2.

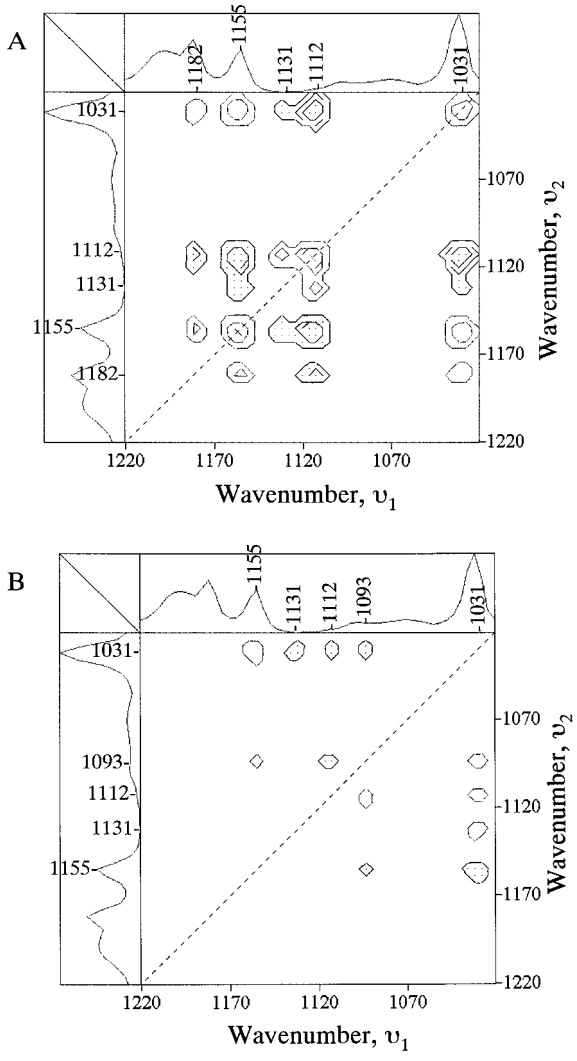

Figure 4. Synchronous (A) and asynchronous (B) 2D FT-Raman correlation spectra in the range 1220−1020 cm^{-1}, constructed from the spectra of PS, SE91, and SE73 (set A).

or Figure 1. It is impossible to assign this band to PS or PPE. However, the spectral region around 1600 cm^{-1} for the blends can only be concerned with the phenyl ring-stretching vibrations. Hence the band may be characteristic of the specific interaction between PS and PPE. It might be a "new" band emerging from blending.

Figure 4A depicts the 2D synchronous FT-Raman correlation spectrum of set A in the range of 1220−1020 cm^{-1}. A band at 1031 cm^{-1} is ascribed to PS (Table 1). The positive cross-peaks at (1182, 1031 cm^{-1}) and (1155, 1031 cm^{-1}) indicate that bands at 1182 and 1155 cm^{-1} are due to PS, while the negative cross-peaks at (1131, 1031 cm^{-1}) and (1112, 1031 cm^{-1}) indicate that bands at 1131 and 1112 cm^{-1} are assigned to PPE. It is noticeable that the band at 1201 cm^{-1} due to PS, which has a significant intensity in the one-dimensional spectrum, does not appear in Figure 4A. The explanation for this disappearance is the same as that for the absence of the bands at 1448 and 1329 cm^{-1} in Figure 3A. In fact, the intensity of the band at 1201 cm^{-1} is 0.05621, 0.05830, and 0.05779 for PS, SE91, and SE73, respectively. It also has an occasional increase, instead of a monotonic decrease, from PS to SE91. Most probably, the band at 1201 cm^{-1} is associated with the conformation change of PS in the blends.

The corresponding asynchronous correlation spectrum is presented in Figure 4B. The relationships between two bands derived from Figure 4B are listed in Table 3. A band at 1093 cm^{-1} does not appear in Figure 4A and Figure 1. From Φ(1155, 1093) < 0, Φ(1031, 1093) < 0 and Φ(1112, 1093) > 0, it is most likely due to PPE. The 9th to 11th rows of Table 3 give asynchronous relationships between the bands at 1131, 1112, and 1093 cm^{-1} due to the CH in-plane deformation of PPE and the band at 1031 cm^{-1} due to the CH in-plane deformation of PS.

Here, we explain the asynchronous peaks at (1131, 1031 cm^{-1}), (1112, 1031 cm^{-1}) and (1093, 1031 cm^{-1}) as reflecting the specific interaction between PS and PPE. The aryl CH in-plane deformations are known to change with even subtle variations in the environment of an aromatic ring. According to the analysis described above, only if the sequential order between the bands in set A is reversed with respect to that in set B, the bands can be regarded as involved in the formation of PS/PPE blends. Table 3 shows that it is seen that the intensity change of the bands at 1131, 1112, and 1093 cm^{-1} occurs at lower PPE contents in comparison with the band at 1031 cm^{-1} in set A. From Table 5, which summarizes the order of intensity variations between two bands for set B, it is seen that the intensity change of the bands at 1131, 1112, and 1093 cm^{-1} takes place at higher PPE content than that of the band at 1031 cm^{-1} in set B. Thus, the bands at 1131, 1112, and 1093 cm^{-1} due to PPE and the band at 1031 cm^{-1} due to PS are symptomatic of the specific interaction between PS and PPE.

The 12th and 13th rows of Table 3 give the sequential order of intensity change obtained from the asynchronous peaks at (1093, 1155 cm^{-1}) and (1031, 1155 cm^{-1}).

Table 5. Synchronous, Asynchronous 2D Correlation Intensities and the Order of Intensity Variations between Two Bands for Set B in the Ranges of 1620−1290 and 1220−1020 cm^{-1}

no.	Φ	Ψ	assignment	order[a]
1	Φ(1614, 1602) < 0	Ψ(1614, 1602) < 0	(PPE, PS)	1614 before 1602 cm^{-1}
2	Φ(1590, 1602) < 0	Ψ(1590, 1602) < 0	(PPE, PS)	1590 before 1602 cm^{-1}
3	Φ(1305, 1602) < 0	Ψ(1305, 1602) < 0	(PPE, PS)	1305 before 1602 cm^{-1}
4	Φ(1583, 1602) > 0	Ψ(1583, 1602) > 0	(PS, PS)	1583 before 1602 cm^{-1}
5	Φ(1378, 1602) < 0	Ψ(1378, 1602) < 0	(PPE, PS)	1378 before 1602 cm^{-1}
6	Φ(1428, 1602) < 0	Ψ(1428, 1602) < 0	(PPE, PS)	1428 before 1602 cm^{-1}
7	Φ(1305, 1309) > 0	Ψ(1305, 1309) < 0	(PPE, PPE)	1305 after 1309 cm^{-1}
8	Φ(1131, 1031) < 0	Ψ(1131, 1031) > 0	(PPE, PS)	1131 after 1031 cm^{-1}
9	Φ(1112, 1031) < 0	Ψ(1112, 1031) > 0	(PPE, PS)	1112 after 1031 cm^{-1}
10	Φ(1093, 1031) < 0	Ψ(1093, 1031) > 0	(PPE, PS)	1093 after 1031 cm^{-1}

[a] ν_1 after (before) ν_2 means the intensity change of the band at ν_1 occurs at higher (lower) PPE contents than that at ν_2.

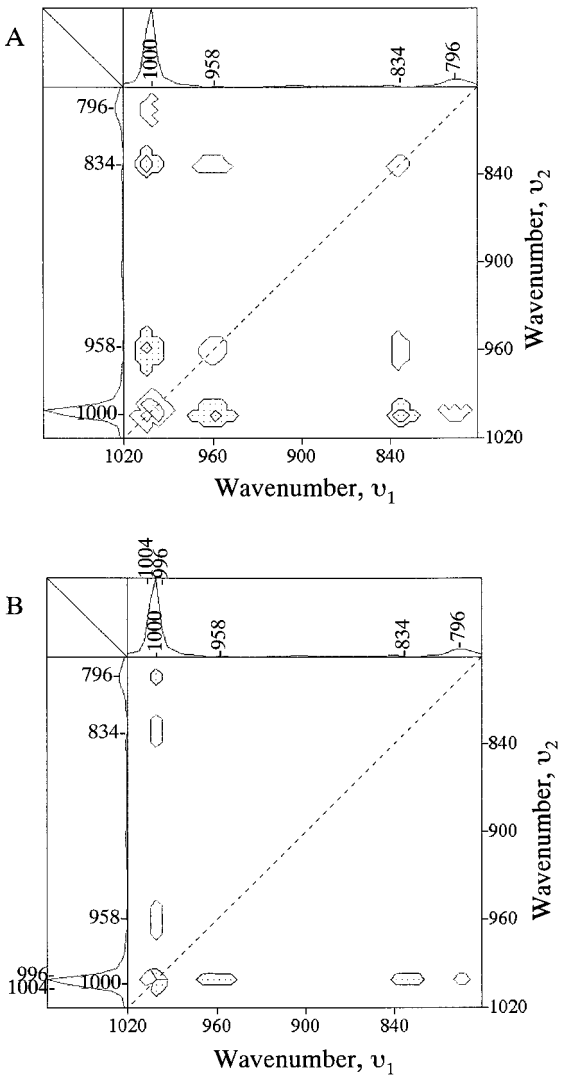

Figure 5. Synchronous (A) and asynchronous (B) 2D FT-Raman correlation spectra in the range 1020−780 cm^{-1}, constructed from the spectra of PS, SE91, and SE73 (set A).

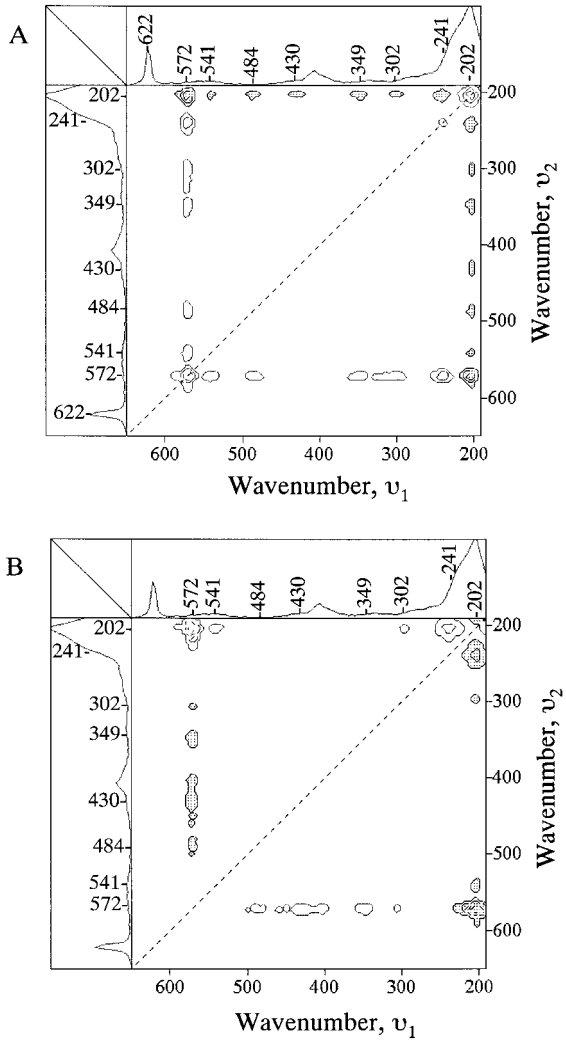

Figure 6. Synchronous (A) and asynchronous (B) 2D FT-Raman correlation spectra in the range 650−190 cm^{-1}, constructed from the spectra of PS, SE91, and SE73 (set A).

These asynchronous peaks cannot be identified for set B (see Figure 8B). The band at 1155 cm^{-1} due to the CH in-plane deformation of PS most probably reflects the conformation change of PS when mixed with PPE.

The synchronous and asynchronous correlation maps for set A in the range of 1020−780 cm^{-1} are shown in parts A and B of Figure 5. A band at 1000 cm^{-1} arises from PS. The positive cross-peak at (1000, 796 cm^{-1}) indicates that a band at 796 cm^{-1} is assigned to PS, while the negative cross-peaks at (1000, 834 cm^{-1}) and (1000, 958 cm^{-1}) suggest that bands at 834 and 958 cm^{-1} are due to PPE.

The relationships between the bands in the asynchronous map are listed in Table 4. The first, second and third rows of Table 4 give asynchronous relationships between the band at 1000 cm^{-1} and the bands at 958, 834, and 796 cm^{-1}. The bands at 958, 834, and 796 cm^{-1} are assigned to CH out-of-plane vibrations of PPE and PS. The band at 1000 cm^{-1} is known as the "Star of David" vibration for a monosubstituted aromatic ring and, thus, is due to the ring-stretching vibration of PS.[38] The corresponding asynchronous peaks among these

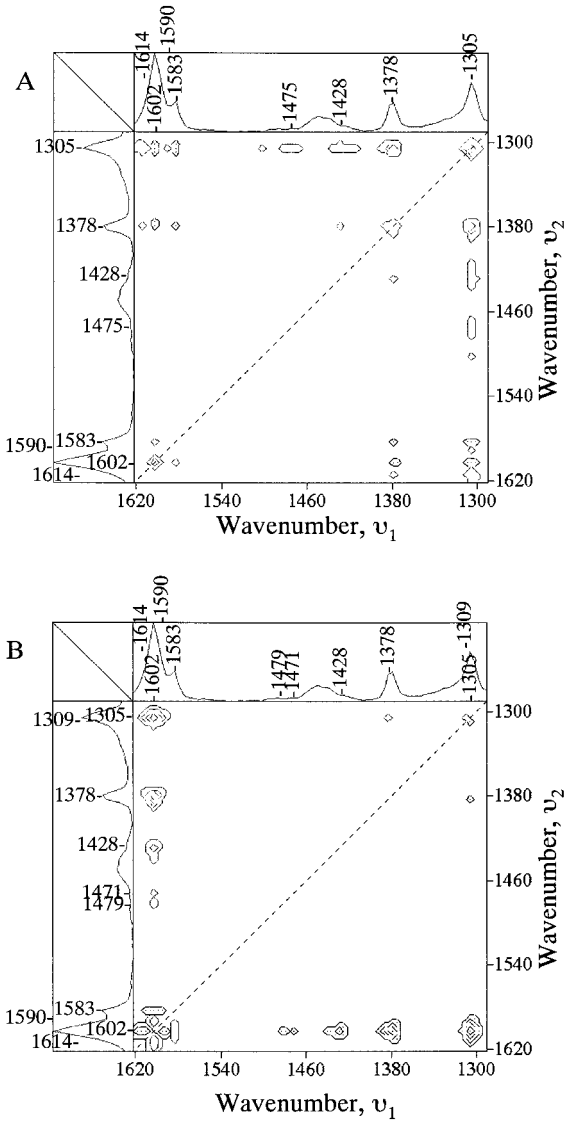

Figure 7. Synchronous (A) and asynchronous (B) 2D FT-Raman correlation spectra in the range 1620−1290 cm^{-1}, constructed from the spectra of SE55, SE37, and SE19 (set B).

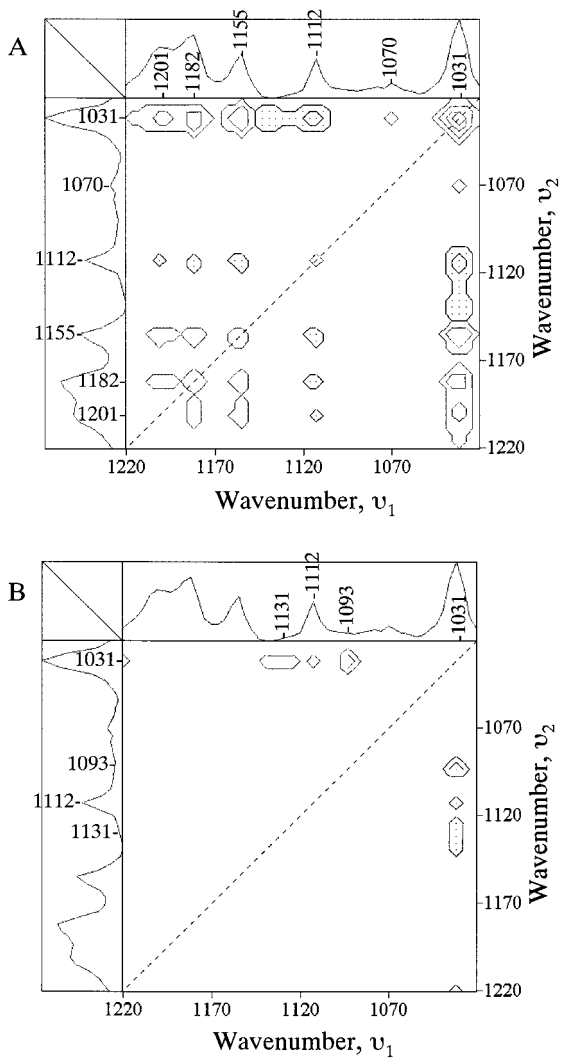

Figure 8. Synchronous (A) and asynchronous (B) 2D FT-Raman correlation spectra in the range 1220−1020 cm^{-1}, constructed from the spectra of SE55, SE37, and SE19 (set B).

bands are not identifiable for set B in Figure 9B. Therefore, there is no evidence that the bands at 958, 834, and 796 cm^{-1} are indicative of the specific interaction. They are indicative of the conformation change in the polymer blends.

It is noted in Figure 5B that three bands are discriminated around 1000 cm^{-1}. Figure 1 shows that PS has a very strong band around 1000 cm^{-1}, and PPE has a very weak band at this spot. The intense Raman band of a monosubstituted aromatic ring around 1000 cm^{-1} accompanies a weak feature due to CH out-of-plane vibration at the lower frequency side.[38] We, therefore, assign the band at 996 cm^{-1} to the CH out-of-plane deformation mode of PS. The band at 1004 cm^{-1} is assigned to the in-plane ring deformation mode of PPE.

The asynchronicity between the bands at 1004 and 1000 cm^{-1} should arise from the specific interaction in the blends since they are due to the ring deformation and stretching modes, respectively. This conclusion is consistent with the conclusions drawn from Figures 4B and 3B. However, the asynchronicity at (996, 1000 cm^{-1}) may only reflect that the band at 996 cm^{-1} is sensitive to the conformation change in the PS/PPE blends.

Figure 6A shows the synchronous correlation spectrum of set A in the range 650−190 cm^{-1}. It is noticeable that bands of PS at 622 and 405 cm^{-1}, which have significant intensities in the one-dimensional spectrum (Figure 1), do not appear in Figure 6A. The intensity of the band at 622 cm^{-1} is 0.04857, 0.04571, and 0.04351 for PS, SE91 and SE73, respectively. While its intensity decreases with the reduction in PS content, the decrease is minimal from SE91 to SE73, in comparison with that from PS to SE91. On the other hand, the band at 405 cm^{-1} experiences occasional increase with the reduction of PS content. In fact, its intensity is 0.01940, 0.02988, and 0.02253 for for PS, SE91 and SE73, respectively. The bands at 622 and 405 cm^{-1} are assigned to in-plane and out-of-plane ring deformation modes, respectively. Therefore, these bands are indicative of the specific interaction between PS and PPE.

The corresponding asynchronous correlation map is shown in Figure 6B. The sixth to ninth rows of Table 4 all give asynchronous relationships between a band at 202 cm^{-1} due to PS and bands at 572, 541, 302, and 241 cm^{-1} due to PPE. The 10th to 13th rows yield relationships between two bands due to PPE. All these bands are assigned to various ring deformation modes of PPE and PS, and the asynchronicity between them

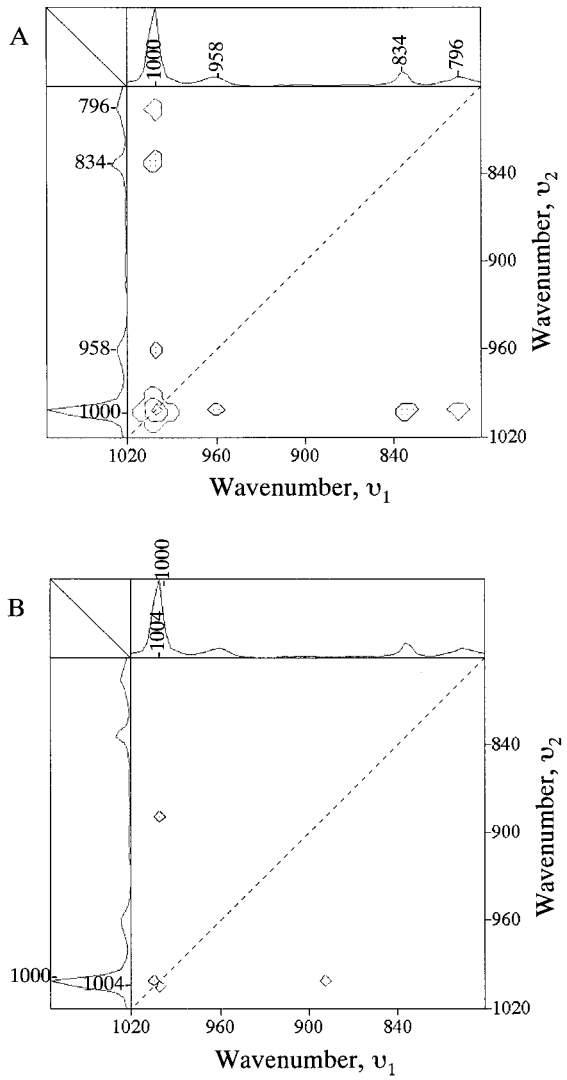

Figure 9. Synchronous (A) and asynchronous (B) 2D FT-Raman correlation spectra in the range 1020−780 cm^{-1}, constructed from the spectra of SE55, SE37, and SE19 (set B).

should reflect the specific interaction between PS and PPE.

4. 2D Correlation Spectra of Set B. The synchronous correlation map of set B in the range of 1620−1290 cm^{-1} is depicted in Figure 7A. It is very similar to the corresponding map for set A in Figure 3A. As in the case of set A, the band at 1448 cm^{-1} due to the methylene bending mode of PS, which has a significant intensity in the one-dimensional reference spectrum, shows no autopeak or cross-peak in the map. The explanation for this absence is also the same as that for set A. (The intensity at 1448 cm^{-1} is 0.03057, 0.03180, and 0.02920 for SE55, SE37 and SE19, respectively.) Thus, the main chain conformation of PS undergoes noticeable changes not only in set A but also in set B.

Figure 7B presents the corresponding asynchronous correlation map. The asynchronicity between the bands at 1614, 1590, and 1305 cm^{-1} due to the ring-stretching modes of PPE and the band at 1602 cm^{-1} due to the ring-stretching mode of PS are shown in the first, second, and third rows of Table 5. The intensity change of the former three bands occurs predominantly at lower PPE content than that of the later band for set B. For set A (Table 3) we have deduced that the intensity change of the bands at 1614, 1590, and 1305 cm^{-1} takes place largely at higher PPE content than that of the band at 1602 cm^{-1}. In both cases, these bands are indicators of the specific interaction in the blends.

The fifth row of Table 5 gives the asynchronicity between the band at 1602 cm^{-1} and the band at 1378 cm^{-1} due to the methyl symmetric deformation of PPE. From Table 5, it is seen that the intensity change of the band at 1378 cm^{-1} occurs at lower PPE content than the band at 1602 cm^{-1} for set B. From Table 3, it is seen that the intensity change of the band at 1378 cm^{-1} occurs at higher PPE contents than the band at 1602 cm^{-1} for set A. The bands at 1378 and 1602 cm^{-1} are indicative of the specific interaction that is common to the blends in set A and set B.

The band around 1305 cm^{-1} of PPE appears as a single band for set A (Figures 3A and 3B). However, it appears at 1309 and 1305 cm^{-1} as two bands in Figure 7B for set B. The intensity change of the band at 1309 cm^{-1} occurs predominantly at lower PPE content than that at 1305 cm^{-1} (the seventh row of Table 5). The band at 1309 cm^{-1}, assigned to a ring-stretching mode of PPE, is unique to set B. We propose that there are two kinds of specific interactions in set B. One is similar to that in set A, as represented by the band at 1305 cm^{-1}, and the other is different from that in set A, as represented by the band at 1309 cm^{-1}.

The band at 1475 cm^{-1}, due to the ring-stretching mode of PPE, which appears as a single band in Figure 3A, also appears as two bands in Figure 7B. The splitting for set B indicates that a new specific interaction takes place in set B.

Figure 8A shows the synchronous correlation map of set B in the range of 1220−1020 cm^{-1}. Note that the map is considerably different from the corresponding map for set A (Figure 4A). Bands at 1201 and 1070 cm^{-1} develop cross-peaks in Figure 8A, but no peak in Figure 4A. The band at 1070 cm^{-1} is assigned to the C−C stretching vibration along the main chain of PS. Thus, the main chain of PS has different conformations in set A and set B. This conclusion can also be derived from the presence of the band at 1201 cm^{-1} in Figure 8A and its absence in Figure 4A.

The sequential order between the bands at 1131, 1112, and 1093 cm^{-1} due to PPE is just opposite to that for set A. (See Tables 3 and 5.) These aryl CH in-plane deformations suggest the existence of the specific interaction common to set A and set B.

The synchronous and asynchronous correlation maps of set B in the range of 1020−780 cm^{-1} are shown in parts A and B of Figure 9. The synchronous map for set B is very close to that for set A. To cut all the noise the threshold for Figure 9B is chosen to be very high. Of note in Figure 9B is the cross-peak at (1004, 1000 cm^{-1}). Interestingly, the sequential order between the band at 1004 cm^{-1} due to PPE and the band at 1000 cm^{-1} due to PS in set B is opposite to that in set A, as is seen by comparing Table 6 with Table 4. The two bands due to the ring-stretching vibrations of PPE and PS are thus indicative of the specific interaction common to set A and set B.

The synchronous correlation map of set B in the range of 650−190 cm^{-1} is shown in Figure 10A. It is very similar to that for set A in the same range. The only difference is that cross-peaks for the band at 622 cm^{-1} due to the in-plane ring deformation of PS appear in

Table 6. Synchronous, Asynchronous 2D Correlation Intensities and the Order of Intensity Variations between Two Bands for Set B in the Ranges of 1020−780 and 650−190 cm^{-1}

no.	Φ	Ψ	assignment	order[a]
1	Φ(1004, 1000) > 0	Ψ(1004, 1000) < 0	(PPE, PS)	1004 after 1000 cm^{-1}
2	Φ(572, 202) < 0	Ψ(572, 202) < 0	(PPE, PS)	572 before 202 cm^{-1}
3	Φ(241, 202) < 0	Ψ(241, 202) < 0	(PPE, PS)	241 before 202 cm^{-1}
4	Φ(314, 202) < 0	Ψ(314, 202) < 0	(PPE, PS)	314 before 202 cm^{-1}
5	Φ(295, 202) < 0	Ψ(295, 202) < 0	(PPE, PS)	295 before 202 cm^{-1}
6	Φ(484, 202) < 0	Ψ(484, 202) < 0	(PPE, PS)	484 before 202 cm^{-1}
7	Φ(449, 572) > 0	Ψ(449, 572) < 0	(PPE, PPE)	449 after 572 cm^{-1}
8	Φ(229, 572) > 0	Ψ(229, 572) > 0	(PPE, PPE)	229 before 572 cm^{-1}

[a] ν_1 after (before) ν_2 means the intensity change of the band at ν_1 occurs at higher (lower) PPE contents than that at ν_2.

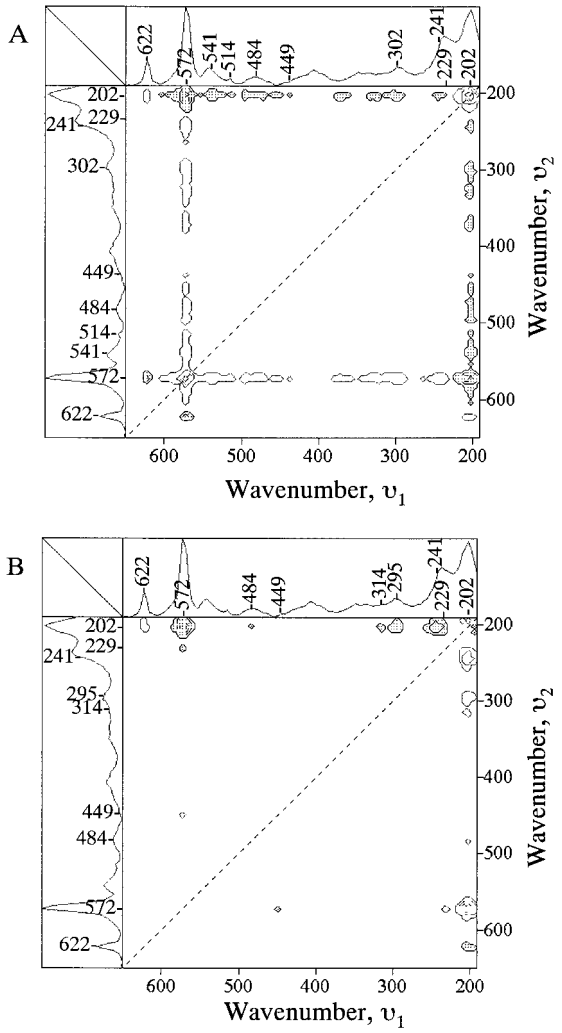

Figure 10. Synchronous (A) and asynchronous (B) 2D FT-Raman correlation spectra in the range 650−190 cm^{-1}, constructed from the spectra of SE55, SE37, and SE19 (set B).

Figure 10A and do not appear in Figure 6A. While in set A this band is indicative of the specific interaction between PS and PPE, there is no evidence that it is indicative of the specific interaction in set B. Thus, the molecular interactions in set A and set B must be different from each other.

The corresponding asynchronous correlation map is presented in Figure 10B. The second and third rows of Table 6 show the sequential orders between the band at 202 cm^{-1} due to PS and the bands at 572 and 241 cm^{-1} due to PPE. These orders in set B are opposite to those in set A, indicating that the bands at 572, 241, and 202 cm^{-1} due to the out-of-plane ring deformations of PS and PPE are indicative of the specific interaction common to set A and set B.

Comparing Figure 10B with Figure 6B, it is seen that the band at 302 cm^{-1} due to PPE in Figure 6B splits into two bands at 314 and 295 cm^{-1} in Figure 10B. The splitting indicates that a new specific interaction appears in set B. Comparison between Figures 6B and 10B also shows that the band at 229 cm^{-1} appears only for set B. Therefore, it is unique to set B and may represent a particular molecular interaction in set B.

Conclusions

Generalized two-dimensional (2D) FT-Raman correlation spectroscopy has been applied to the study of the conformational changes and specific interactions in blends of atactic PS and PPE. Six FT-Raman spectra of PS/PPE blends have been divided into two narrow windows for the 2D correlation analysis: set A (PS/PPE = 100/0, 90/10, 70/30) and set B (PS/PPE = 50/50, 30/70, 10/90).

In the present study the interaction spectra of the blends have been investigated in detail to assist the 2D correlation analysis. The 2D synchronous correlation analysis separates the bands of PS from those of PPE and detects bands that are not identifiable from the one-dimensional spectra of PS and PPE. While only one band at 1604 cm^{-1} is observed in the one-dimensional spectrum of PPE, two bands are identified at 1614 and 1590 cm^{-1} in the synchronous spectrum. The synchronous correlation analysis also reveals a significant change in the main chain conformation of PS in set A and set B, based on the abnormal behavior of the bands at 1448 and 1329 cm^{-1} due to the methylene vibrations, of the band at 1070 cm^{-1} due to the C−C stretching vibration, and of the band at 1201 cm^{-1} due to the aryl CH wag vibration.

The 2D asynchronous correlation analysis shows many out-of-phase band variations that have opposite trends in set A and set B. Such out-of-phase variations have been explained as characteristic features of the specific interaction that is common to the blends in set A and set B. The bands at 1614, 1590, 1305, 1004, 572, and 241 cm^{-1} due to PPE and those at 1602, 1000, and 202 cm^{-1} due to PS are found to be indicative of this specific interaction in the PS/PPE blends. The bands at 1131, 1112, and 1093 cm^{-1} due to the aryl CH in-plane deformations of PPE and the band at 1031 cm^{-1} due to the corresponding mode of PS are also indicative of the specific interaction common to sets A and B. Therefore, the phenyl rings of both PS and PPE should be involved in the formation of the blends. In addition, the band at 1378 cm^{-1} due to the methyl symmetric deformation of PPE is indicative of the specific interaction common to set A and set B, suggesting that the methyl groups of PPE are also involved in the blend formation. It is speculated that the phenylene ring of PPE with two methyl groups can have more favorable interaction with

the phenyl ring of PS.

Set A and set B also contain molecular interactions different from each other. The band at 1606 cm^{-1} is unique to set A, while those at 1309 and 229 cm^{-1} are observed only for set B, representing the particular interaction in set A and set B, respectively. The different molecular interaction is also reflected in the splitting of the band at 1475 cm^{-1} of set A into two bands at 1479 and 1471 cm^{-1} of set B, and in the splitting of the band at 302 cm^{-1} of set A into two bands at 314 and 295 cm^{-1} of set B.

We have explained any asynchronicity between two bands due to ring-stretching or deformation modes as caused by the specific interaction in the polymer blends, since these bands are influenced only by strong interactions. The asynchronicity between these bands detected both in set A and in set B always has opposite trends, and has been explained as feature of the specific interaction common to set A and B. The asynchronicity between these bands which is detected only in set A (or B) has been explained as symptomatic of the particular interactions in set A (or B).

Except for the case outlined above, the asynchronicity between bands due to aryl CH wag modes has been explained as an evidence for the chain conformation change of PS and PPE when mixed together. The bands at 1155, 996, and 796 cm^{-1} due to the aryl CH wagging vibrations of PS are indicative of the conformation change of PS, while the bands at 958 and 834 cm^{-1} due to the aryl CH wagging vibrations of PPE are indicative of the conformation change of PPE.

The 2D asynchronous analysis is a powerful tool in analyzing the highly overlapped region around 1000 cm^{-1} in the spectra of the blends. It assigns the band at 1004 cm^{-1} to the in-plane ring deformation mode of PPE (ν_{12}), the band at 1000 cm^{-1} to that of PS (ν_{12}), and the band at 996 cm^{-1} to the out-of-plane CH deformation mode of PS (ν_5).

In summary, generalized 2D correlation spectroscopy enables one to study the molecular interactions in polymer blends. The feasibility has been demonstrated in our previous paper,[41] where six NIR spectra of the PS/PPE blends have been used for 2D correlation. In a future paper we will report the interesting 2D correlation results obtained by using three NIR spectra of the blends.

Acknowledgment. This work was supported by a Grant-in-Aid to Y. Ozaki (09640616) from the Ministry of Education, Science, and Culture, Japan.

References and Notes

(1) Noda, I. *Appl. Spectrosc.* **1993**, *47*, 1329.
(2) Noda, I. *Bull. Am. Phys. Soc.* **1986**, *31*, 520.
(3) Noda, I. *J. Am. Chem. Soc.* **1989**, *111*, 8116.
(4) Noda, I. *Appl. Spectrosc.* **1990**, *44*, 550.
(5) Ozaki, Y.; Noda, I. *J. Near Infrared Spectrosc.* **1996**, *4*, 85.
(6) Gustafson, T.; et al. In *Time-Resolved Vibrational Spectroscopy V*; Lau, A., Siebert, F., Eds.; Springer-Verlag: Berlin, 1994; pp 131−135.
(7) Noda, I.; Liu, Y.; Ozaki, Y.; Czarnecki, M. A. *J. Phys. Chem.* **1995**, *99*, 3068.
(8) Nabet, A.; Pezolet, M. *Appl. Spectrosc.* **1997**, *51*, 466.
(9) Liu, Y.; Ozaki, Y.; Noda, I. *J. Phys. Chem.* **1996**, *100*, 7327.
(10) Noda, I.; Liu, Y.; Ozaki, Y. *J. Phys. Chem.* **1996**, *100*, 8665.
(11) Noda, I.; Liu, Y.; Ozaki, Y. *J. Phys. Chem.* **1996**, *100*, 8674.
(12) Ozaki, Y.; Liu, Y.; Noda, I. *Macromolecules* **1997**, *30*, 2391.
(13) Wang, Y.; Murayama, K.; Myojo, Y.; Tsenkova, R.; Hayashi, N.; Ozaki, Y. *J. Phys. Chem. B* **1998**, *102*, 6655.
(14) Müller, M.; Buchet, R.; Fringeli, U. P. *J. Phys. Chem.* **1996**, *100*, 10810.
(15) Sefara, N. L.; Magtoto, N. P.; Richardson, H. H. *Appl. Spectrosc.* **1997**, *51*, 536.
(16) Gericke, A.; Gadaleta, S. J.; Brauner, J. W.; Mendelsohn, R. *Biospectroscopy* **1996**, *2*, 353.
(17) Czarnecki, M. A.; Wu, P.; Siesler, H. W. *Chem. Phys. Lett.* **1998**, *283*, 326.
(18) Czarnecki, M. A.; Maeda, H.; Y. Ozaki; Suzuki, M.; Iwahashi, M. *J. Phys. Chem. A* **1998**, *102*, 9117.
(19) Schultz, C. P.; Fabian, H.; Mantsch, H. H. *Biospectroscopy* **1998**, *4*, 19.
(20) Ren, Y.; Shimoyama, M.; Ninomiya, T.; Matsukawa, K.; Inoue, H.; Noda, I.; Ozaki, Y. *Applied Spectroscopy*, submitted for publication.
(21) Hendra, P. J.; Johes, C. H.; Warnes, G. *Fourier Transform Raman Spectroscopy, Instrumentation and Chemical Applications;* Ellis Horwood: Chichester, England, 1991.
(22) Schrader, B. In *Practical Fourier Transform Infrared Spectroscopy;* Ferraro, J. R., Krishnan, K., Eds.; Academic Press: San Diego, CA, 1990.
(23) Hendra, P. J.; Agbenyega, J. K. *The Raman Spectra of Polymers*; John Wiley & Sons: Chichester, England, 1993.
(24) Koenig, J. L. *Spectroscopy of Polymers*; American Chemical Society: Washington, DC, 1992; p 125.
(25) Dong, J.; Ozaki, Y.; Nakashima, K. *Macromolecules* **1997**, *30*, 1111.
(26) Dong, J.; Ozaki, Y. *Macromolecules* **1997**, *30*, 286.
(27) Fawcett, A. H. *Polymer Spectroscopy;* John Wiley & Sons: Chichester, England, 1996.
(28) Jo, W. H.; Cruz, C. A.; Paul, D. R. *J. Polym. Sci., Part B: Polym. Phys.* **1989**, *27*, 1057.
(29) Koenig, J. L.; Tovar, M. J. M. *Appl. Spectrosc.* **1981**, *35*, 543.
(30) Coleman, M. M.; Graf, J. F.; Painter, P. C. *Specific Interactions and the Miscibility of Polymer Blends;* Technomic Publishing: Lancaster, PA, 1991.
(31) Utracki, L. A. *Polymer Alloys and Blends, Thermodynamics and Rheology;* Carl Hanser: Munich, Germany, 1989.
(32) Wellinghoff, S. T.; Koenig, J. L.; Baer, E. *J. Polym. Sci.: Polym. Phys.* **1977**, *15*, 1913.
(33) Shultz, A. R.; Gendron, B. M. *J. Appl. Polym. Sci.* **1972**, *6*, 461.
(34) Wellinghoff, S. T.; Baer, E. *Prepr. Am. Chem. Soc., Div. Org. Coatings Plast. Chem.* **1976**, *36*, 140.
(35) Palmer, R. A.; Gregoriou, V. G.; Chao, J. L. *Polym. Prepr. (Am. Chem. Soc., Div. Polym. Chem.)* **1992**, *33*, 1222.
(36) Boscoletto, A. B.; Checchin, M.; Tavan, M.; Camino, G.; Costa, L.; Luda, M. P. *J. Appl. Polym. Sci.* **1994**, *53*, 121.
(37) Djordjevic, M. B.; Porter, R. S. *Polym. Prepr. (Am. Chem. Soc., Div. Polym. Chem.)* **1981**, *22*, 323.
(38) Dollish, F. R.; Fateley, W. G.; Bentley, F. F. *Characteristic Raman Frequencies of Organic Compounds*; Wiley: New York, 1974.
(39) Lin-Vien, D.; Colthup, N. B.; Fateley, W. G.; Grasselli, J. G. *Infrared and Raman Characteristic Frequencies of Organic Molecules*; Academic Press Inc.: San Diego, CA, 1991.
(40) Nyquist, R. A.; Putzig, C. L.; Leugers, M. A.; McLachlan, R. D.; Thill, B. *Appl. Spectrosc.* **1992**, *46*, 981.
(41) Ren, Y.; Ozaki. Y.; Murakami, T.; Nishioka, T.; Nakashima, K. *Macromol. Symp.*, in press.

MA990072E